Relativistic multiconfiguration method in low-energy scattering of electrons from xenon atoms

P. Syty[a,*], J.E. Sienkiewicz[a], S. Fritzsche[b]

[a] *Department of Theoretical Physics and Mathematical Methods, Gdańsk University of Technology, ul. Narutowicza 11/12, 80-952 Gdańsk, Poland*
[b] *Fachbereich Physik, Universität Kassel, Heinrich-Plett-Str. 40, D-34132 Kassel, Germany*

Abstract

The elastic scattering of slow electrons from xenon atoms is calculated in a relativistic multiconfiguration method. The correlation effects responsible for target polarization are treated in a relativistic configuration-interaction scheme that allows for dynamics effects. Calculations of the spin polarization and differential cross sections are discussed and compared with experimental and other theoretical data.
© 2003 Elsevier Science Ltd. All rights reserved.

Keywords: Elastic scattering of electrons from Xenon; Multiconfiguration Dirac–Fock method; Differential cross section; Spin polarization

1. Introduction

In the last years, the scattering of slow electrons by atoms has been extensively studied by both experimentalists and theoreticians. From the theoretical point of view, the difficulties arise from the need for precise calculations of target polarization. Present calculations have been performed by using the relativistic version of the multiconfiguration and CI approach (Sienkiewicz et al., 1995; Sienkiewicz and Baylis, 1997). The method allows for describing the polarization of different target states due to the incoming electron charge through bound relativistic configuration expansions. The polarization is different for different kinetic energies of the incident electron, and thus dynamic effects are taken into account. The relativistic phase shifts obtained by this method are used to calculate spin polarization and differential cross sections of electron scattering by xenon in its ground state at a few selected energies.

A review of the theory used in computations is presented in Section 2 and the computational procedure is described in Section 3. Our results are presented and compared with experiment and other available calculations in Section 4. At last, the conclusion remarks are included in Section 5.

2. Theory

Let us start from the relativistic scattering equation

$$H_{N+1}\Psi = \mathscr{E}\Psi. \tag{1}$$

Here, H_{N+1} is the $(N + 1)$-electron Dirac–Coulomb Hamiltonian operator

$$H_{N+1} = \sum_{i=1}^{N+1} \left[c \sum_{k=1}^{3} \alpha_k^i p_k^i + (\beta^i - 1)c^2 - \frac{Z}{r_i} \right] + \sum_{i=1}^{N+1} \sum_{j=i+1}^{N+1} \frac{1}{r_{ij}}, \tag{2}$$

and Ψ is the scattering state wavefunction including one electron in the continuum.

The total energy of the scattering system is

$$\mathscr{E} = E_a + E, \tag{3}$$

where E_a is the energy of the N-electron target and E is the kinetic energy of the scattered electron.

*Corresponding author.
 E-mail address:* sylas@task.gda.pl (P. Syty).

To obtain the approximate solution of our scattering equation (1), we use the multiconfiguration Dirac–Fock method. In this method, an atomic state function (ASF) is approximated by a linear combination of configuration symmetry functions (CSFs),

$$\Phi_a(P_a J_a M_a) = \sum_{r=1}^{n_c} b_{ar}\phi_r(N, \gamma_r J_a M_a P_a), \qquad (4)$$

where P_a is the parity of the atomic state, J_a is the total angular momentum and M_a the magnetic number, and n_c—the number of CSFs. The CSFs are eigenfunctions of the parity and the total angular momentum operators and are associated with the set of the quantum numbers (PJM). They are built from antisymmetrized products of a common set of orthonormal Dirac orbitals

$$u_{n\kappa m}(\mathbf{r}) = \frac{1}{r}\begin{pmatrix} P_{n\kappa}(r)\chi_{\kappa m}(\mathbf{r}/r) \\ iQ_{n\kappa}(r)\chi_{-\kappa m}(\mathbf{r}/r) \end{pmatrix}, \qquad (5)$$

where P_{nk} and Q_{nk} are the large and small components of the Dirac radial spinor, respectively, and the spin-angular function is given by

$$\chi_{\kappa m}(\mathbf{r}/r) = \sum_{\sigma=\pm 1/2} \langle jm|l,\tfrac{1}{2},m-\sigma,\sigma\rangle Y_l^{m-\sigma}(\mathbf{r}/r)\chi_{1/2}^\sigma. \quad (6)$$

Here, $\langle jm|l,\tfrac{1}{2},m-\sigma,\sigma\rangle$ is a Clebsch–Gordan coefficient, $Y_l^{m-\sigma}(\mathbf{r}/r)$ is a spherical harmonic, $\chi_{1/2}^\sigma$ is the spin eigenfunction, κ is the relativistic angular quantum number, $\kappa = \pm(j+\tfrac{1}{2})$ for $l = j\pm\tfrac{1}{2}$, where j is the total angular momentum and l is the orbital quantum number.

The symbol γ_r in Eq. (4) denotes the occupation and the coupling of the electron subshells, and thus allows us to distinguish CSFs of the same global symmetry. The radial parts of the functions $\phi_r(N, \gamma_r J_a M_a P_a)$ as well as the mixing coefficients b_{ar} are generated in the SCF process with respect to the Dirac–Coulomb Hamiltonian.

We express the total wave function of the $(N+1)$-electron scattering system in the form (Burke et al., 1971)

$$\Psi(PJM; N+1) = \mathcal{A}\sum_{a=1}^{m_a} c_a\Phi_a(P_a J_a M_a; N)u_{\kappa(a)m(a)}$$
$$+ \sum_{j=1}^{m_d} d_j\phi_j(PJM; N+1). \qquad (7)$$

The first term on the right-hand side of the above equation is the antisymmetrized product of the bound configuration states of the target atom and one-electron continuum spinors $u_{\kappa(a)m(a)}$.

The continuum Dirac spinor is defined as

$$u_{\kappa m}(\mathbf{r}) = \frac{1}{r}\begin{pmatrix} P_\kappa(r)\chi_{\kappa m}(\mathbf{r}/r) \\ iQ_\kappa(r)\chi_{-\kappa m}(\mathbf{r}/r) \end{pmatrix}, \qquad (8)$$

where now P_k and Q_k refer to continuum orbitals.

The continuum orbitals are solutions of the Dirac–Fock equations

$$\left(\frac{d}{dr} + \frac{\kappa}{r}\right)P_\kappa(r) - \left(2c - \frac{E}{c} + \frac{V(r)}{cr}\right)Q_\kappa(r) = -\frac{X^{(P)}(r)}{r}, \qquad (9)$$

$$\left(\frac{d}{dr} - \frac{\kappa}{r}\right)Q_\kappa(r) + \left(-\frac{E}{c} + \frac{V(r)}{cr}\right)P_\kappa(r) = \frac{X^{(Q)}(r)}{r}. \qquad (10)$$

Here, c is the speed of light, and E is the kinetic energy of the scattered electron. Direct and exchange potentials, $V(r)$ and $X(r)$, are given by Grant et al. (1980). These equations are solved by the method of outward integration.

The first sum in Eq. (7) ranges over all m_a open channels Φ_a. In the case of elastic scattering, we have only one open channel, thus $m_a = 1$.

The second sum in expansion (7) accounts for correlation effects between the scattered electron and the bound target electrons. In our approach, the $(N+1)$-electron configuration state functions ϕ_j are constructed from bound-state orbitals of the target atoms, including excitations of some of the core electrons into a set of virtual orbitals.

In the case of elastic scattering, we obtain the coefficients d_j by solving the system of m_d linear equations

$$\langle \mathcal{A}\Phi u_{\kappa m}|H_{N+1} - \mathcal{E}|\phi_{j'}\rangle$$
$$+ \sum_{j=1}^{m_d} d_j^*\langle \phi_j|H_{N+1} - \mathcal{E}|\phi_{j'}\rangle = 0, \quad j' = 1,\ldots,m_d. \qquad (11)$$

This set of equations is derived by applying the condition that the functional $\langle \Psi|H_{N+1} - \mathcal{E}|\Psi\rangle$ must be stationary with respect to variations of the d_j coefficients.

The solution of Eq. (11) determines new direct and exchange potentials and, through the Dirac–Fock equations (10), an improved continuum scattering orbital. This, in turn, can be used in a new calculation of coefficients d_j. The procedure is iterated to self-consistency.

Now let us define two complex scattering amplitudes $f(\vartheta)$ (the direct amplitude) and $g(\vartheta)$ (the "spin-flip" amplitude), according to Kessler (1985):

$$f(\vartheta) = \frac{1}{2ik}\sum_l \{(l+1)[\exp(2i\delta_l^+) - 1]$$
$$+ l[\exp(2i\delta_l^-) - 1]\}P_l(\cos\vartheta), \qquad (12)$$

$$g(\vartheta) = \frac{1}{2ik}\sum_l [\exp(2i\delta_l^-) - \exp(2i\delta_l^+)]P_l^1(\cos\vartheta), \qquad (13)$$

where ϑ is the scattering angle, $P_l(\cos\vartheta)$ and $P_l^1(\cos\vartheta)$ are the Legendre polynomial and the Legendre

associated function, respectively. The $\delta_l^{\pm}$ are the relativistic phase shifts, where the index $+$ refer to the solution with $\kappa = -l - 1$ and $-$ to the solution with $\kappa = l$.

Having the scattering amplitudes, we can calculate the set of observables—the differential cross section

$$\sigma(\vartheta) = |f(\vartheta)|^2 + |g(\vartheta)|^2 \tag{14}$$

and the spin polarization parameters

$$S(\vartheta) = \frac{i(f(\vartheta)g(\vartheta)^* - f(\vartheta)^*g(\vartheta))}{\sigma(\vartheta)}, \tag{15}$$

$$T(\vartheta) = \frac{|f(\vartheta)|^2 - |g(\vartheta)|^2}{\sigma(\vartheta)}, \tag{16}$$

$$U(\vartheta) = \frac{f(\vartheta)g(\vartheta)^* + f(\vartheta)^*g(\vartheta)}{\sigma(\vartheta)}. \tag{17}$$

These parameters are not independent, since $S + T + U = 1$.

3. Computational procedure

To represent the atomic ground state of the xenon atom, we included 4582 relativistic configuration state functions with the total angular momentum 0 and even parity. These configuration states have been obtained by the excitations of one or two electrons from the 5s and 5p subshells into the set of virtual orbitals 5d 6s 6p 6d 7s 7p 8s 8p 9s 10s. The calculated eigenenergy of the ground state of xenon is -7438.98347 Hartree. The contribution from the relativistic (transverse) Breit interaction between electrons has been added to the Hamiltonian matrix as a perturbation, to obtain a full Dirac–Coulomb–Breit matrix.

The atomic ground-state function and the set of configuration state functions are generated with the atomic structure program GRASP92 written by Parpia et al. (1996).

To construct the total scattering state Ψ and to generate the continuum orbitals $u_{\kappa m}$, we use the computer code COWF developed by Fritzsche (2002).
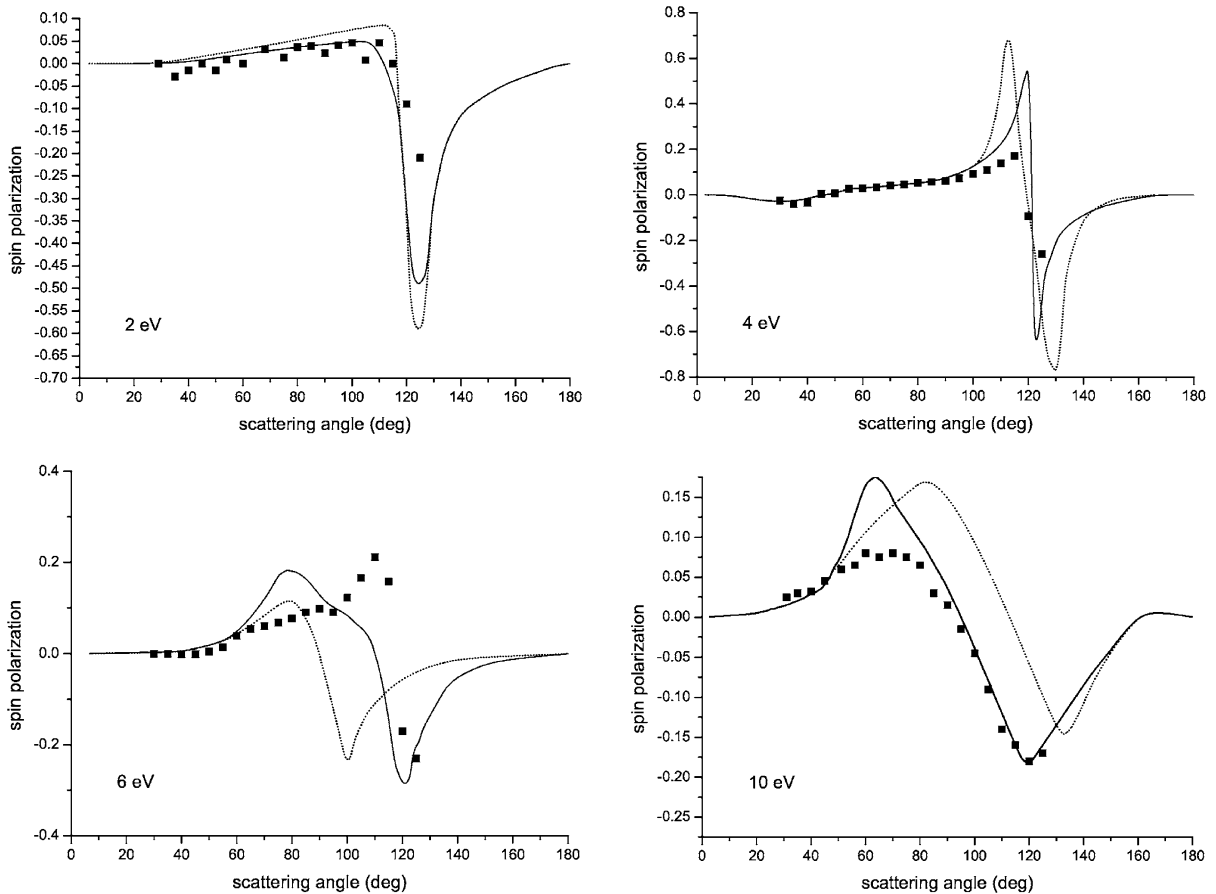

Fig. 1. Spin polarization at 2, 4, 6 and 10 eV against scattering angle. Solid line—present results; dashed line—present results without target polarization; full squares—experimental results of Dümmler et al. (1995).

The original COWF code has been improved and modified to run on multiprocessor computers (Dziedzic et al., 2002). The continuum orbitals are orthogonalized to the atomic orbitals by the Schmidt orthogonalization procedure.

The dominant contribution to the total dipole polarization is from the polarization of the 5s and 5p orbitals. In our calculations we included the dipole polarization of the target xenon atom through the configuration-interaction procedure. The bound $(N + 1)$-electron configuration state functions that account for the dipole polarization are built of atomic orbitals $1s, 2p, \ldots$ up to the $6d$, obtained by the relativistic multiconfiguration self-consistent field method.

Relativistic phase shifts $\delta_l^{\pm}$ are obtained by comparing the numerical solutions with the asymptotic ones at large r:

$$\frac{P_\kappa(r)}{r} \sim j_l(kr) \cos \delta_l^{\pm} - n_l(kr) \sin \delta_l^{\pm}. \tag{18}$$

where $j_l(kr)$ and $n_l(kr)$ are the Bessel and Neumman spherical functions, respectively.

We calculated the relativistic phase shifts $\delta_l^{\pm}$ for $l = 0, 1, \ldots, 10$. For higher values of the orbital momentum (up to $l = 50$), we estimated phase shifts by using the non-relativistic formula of Ali and Fraser (1977).

4. Results

Fig. 1 shows our results for spin polarization at impact energies of 2, 4, 6 and 10 eV, together with the experimental data of Dümmler et al. (1995). For comparison, approximations without target polarization are also presented. In general, our results stay in a good agreement with experimental data. The remaining discrepancies, especially for 6 eV, can be explained by neglecting the influence of inelastic channels in our calculations.

In Fig. 2 we present our results for 10 eV again, but now compared with more theoretical and experimental data than included on the previous figure. The theoretical ones are given by Sienkiewicz et al. (1995) and McEachran and Stauffer (1986). The experimental data are given by Dümmler et al. (1995) and Klewer et al. (1979). For the angles up to the $80°$, our line is closer to the latter experimental points, and for higher angles, to the results of Dümmler et al. (1995).

In Fig. 3 we show our result for differential cross section at a lower energy, 0.67 eV. We compare our result with theoretical and experimental data by Gibson et al. (1988) and the other experimental data given by Weyhreter et al. (1988). One can see that our method is suitable even for energies of the scattered electron below 1 eV.

5. Conclusions

Relativistic multiconfiguration calculations have been performed for the elastic scattering of slow electrons by xenon. The method used in calculations allows for taking into account dynamic effects in a precise ab initio manner through the $(N + 1)$-electron bound configurations. The remaining differences between theoretical and
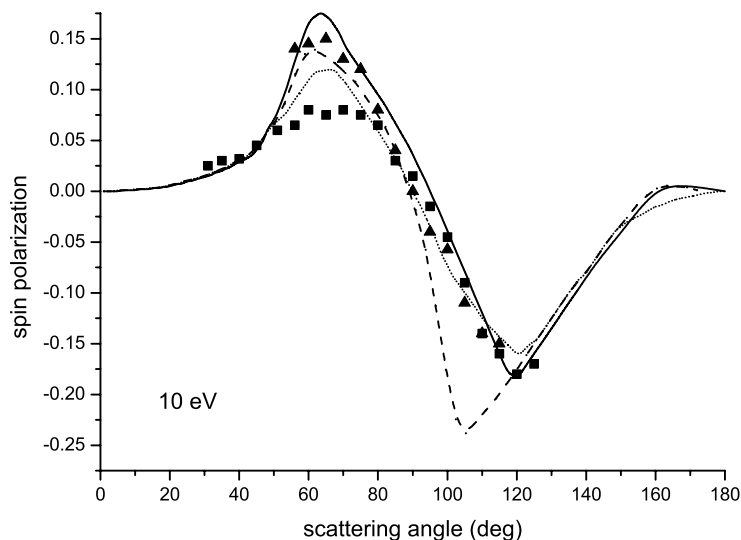

Fig. 2. Spin polarization at 10 eV against scattering angle. Solid line—present results; dashed line—theoretical results of Sienkiewicz et al. (1995); dotted line—theoretical results of McEachran and Stauffer (1986); full squares—experimental results of Dümmler et al. (1995); full triangles—experimental results of Klewer et al. (1979).
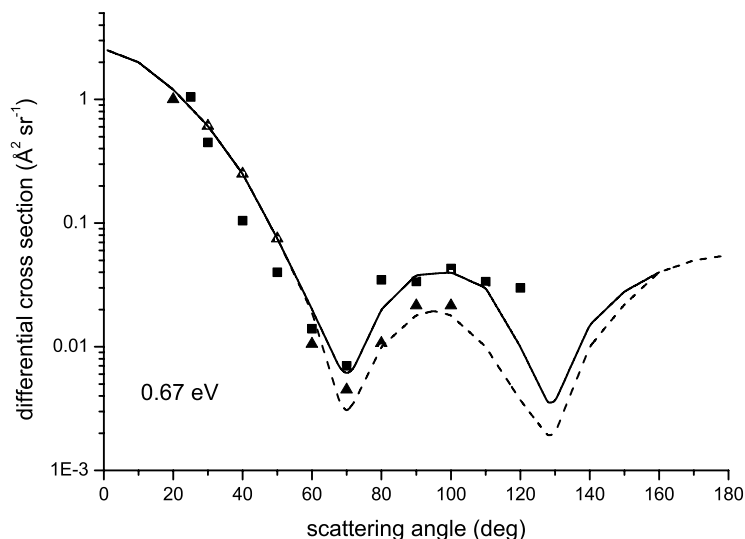
Fig. 3. Differential cross section at 0.67 eV versus scattering angle. Solid line—present results; dashed line—theoretical results of Gibson et al. (1988); full squares—experimental results of Weyhreter et al. (1988); full triangles—experimental results of Gibson et al. (1988).

experimental results arise mainly from neglecting inelastic channels in our computations.

References

Ali, M.A., Fraser, P.A., 1977. The contribution of long-range forces to low-energy phase-shifts. J. Phys. B 10, 3091–3104.

Burke, P.G., Hibbert, A., Robb, W.D., 1971. Electron scattering by complex atoms. J. Phys. B 4, 153–161.

Dümmler, M., Hanne, G.F., Kessler, J., 1995. Left–right asymmetries in elastic and inelastic scattering of polarized electrons from argon, krypton and xenon atoms. J. Phys. B 28, 2985–3001.

Dziedzic, J., Syty, P., Sienkiewicz, J.E., 2002. In preparation.

Fritzsche, S., 2002. In preparation.

Gibson, J.C., Lun, D.R., Allen, L.J., McEachran, R.P., Parcell, L.A., Buckman, S.J., 1988. Low-energy electron scattering from xenon. J. Phys. B 31, 3949–3964.

Grant, I.P., McKenzie, B.J., Norrington, P.H., Mayers, D.F., Pyper, N.C., 1980. An atomic multiconfiguration Dirac–Fock package. Comput. Phys. Commun. 21, 207–231.

Kessler, J., 1985. Polarized Electrons, 2nd Edition. Springer, Berlin, p. 35.

Klewer, M., Beerlage, M.J.M., van der Wiel, M.J., 1979. The polarisation of electrons elastically scattered from xenon at energies between 5 and 300 eV. J. Phys. B 12, 3935–3946.

McEachran, R.P., Stauffer, A.D., 1986. Spin polarization of electrons elastically scattered from xenon. J. Phys. B 19, 3523–3538.

Parpia, F.A., Fischer, C.F., Grant, I.P., 1996. GRASP92: A package for large-scale relativistic atomic structure calculations. Comput. Phys. Commun. 94, 249–271.

Sienkiewicz, J.E., Baylis, W.E., 1997. Relativistic multiconfiguration approach to the spin polarization of slow electrons elastically scattered from krypton. Phys. Rev. A 55, 1108–1112.

Sienkiewicz, J.E., Fritzsche, S., Grant, I.P., 1995. Relativistic configuration-interaction approach to the elastic low-energy scattering of electrons from atoms. J. Phys. B 28, L633–L636.

Weyhreter, M., Barzick, B., Mann, A., Linder, F., 1988. Measurements of differential cross sections for e–Ar, Kr, Xe scattering at E = 0.05–2 eV. Z. Phys. D 7, 333–347.